Degradation of textile dye mixture by heterogeneous photocatalysis employing neural network modeling

Mayane D'albuquerque Irineu, Ramon Vinícius Santos de Aquino, Ada Azevedo Barbosa, Welenilton José do Nascimento Júnior, Josivan Pedro da Silva, Jose Geraldo Andrade Pacheco, Otidene Rossiter Sá da Rocha*

Chemical Engineering Department, Universidade Federal de Pernambuco (UFPE), Av. Prof. Arthur de Sá, s/n, Recife-PE, Brazil, emails: otidene@hotmail.com (O.Ro.Sá da Rocha), mayaneirineu@hotmail.com (M.D. Irineu), viniciusramon59@gmail.com (R.V.S. de Aquino), adabarbosa@hotmail.com (A.A. Barbosa), welenilton@gmail.com (W.J. do Nascimento Júnior), josivan_silva@hotmail.com (J.P. da Silva), jose.pacheco@ufpe.br (J.G.A. Pacheco)

ABSTRACT

This paper investigated the removal of erythrosine (ER) and Fast Green FCF (FG) in binary samples by heterogeneous photocatalysis with ZnO and H_2O_2 and modeled the kinetics of the process by artificial neural networks. Initially, a set of assays were carried out and 93% and 77% degradation rates were achieved for aromatics and color, respectively, after 90 m in the $ZnO/H_2O_2/UV$-C process. The initial concentrations of ZnO, H_2O_2, and pH were investigated in a 2^3-experimental design and the best removal rates were achieved at the central point conditions. Conventional modeling revealed a reasonable fitting by the pseudo-first-order kinetics model ($R^2 > 0.98$) and the kinetic rate constants were estimated at 0.0296 and 0.0141 m^{-1} for color and aromatic content, respectively. An artificial neural network model presented a broader mathematical approach to the kinetics of the process with high R^2 (0.98). A removal of 45% and 58% in total organic carbon and chemical oxygen demand, respectively, was observed. In toxicity assays with lettuce seeds, the absence of inhibition in root growth index (0.85) when exposed to treated samples pointed out the considerable decrease in acute toxicity. Thus, ZnO/H_2O_2 under UV-C radiation was demonstrated to be efficient in removing synthetic dyes from binary samples.

Keywords: Artificial neural network; Dye degradation; Photocatalysis; Toxicity assays

1. Introduction

Industrial development has been considered one of the main causes of current environmental issues. Commercial synthetic dyes are widely employed as raw materials in the manufacturing processes of textile, paper, food and in the pharmaceutical industries [1]. In the food industry, synthetic dyes are able to enhance the visual aspect of the products due to the presence of chromophore groups in their chemical structure. According to the nature of these groups, they may be azo, triarylmethane, indigoid, and xanthene dyes. Erythrosine from the group of the xanthenes, and Fast Green FCF, a triarylmethane, are widely employed in formulating candies, jams, and drinks, among other products [2,3].

Synthetic organic dyes normally display complex aromatic structures, high chemical stability, and low biodegradability, which make them difficult to be removed from residual waters [4]. The high loads of organic dyes in water bodies hinder solar light absorption, therefore, inhibiting

---

* Corresponding author.

the growth of microorganisms by photosynthesis. Besides that, the rise of organic matter also alters the oxygen dissolution in water [5]. Synthetic dyes may also present carcinogenic and mutagenic properties to living beings [6].

Nowadays it is estimated that 10%–15% of dyes are released into the environment without proper treatment [7,8]. The coloration of wastewater is a consequence of process inefficiency and has attracted the attention of researchers worldwide. These chemical complex structures may lead to resistance to aerobic treatments and the generation of hazardous by-products under anaerobic treatment. These by-products may present high toxicity and carcinogenesis. Thus, biological treatments have proven not to be an efficient approach to the mitigation of these substances in wastewater [9].

A range of physico-chemical techniques has been studied for the removal of color in aquatic samples. Adsorption and coagulation/flocculation, for example, are known as simple operations although they only alter the pollutants phase causing secondary pollution. Membrane processes are, in general, highly costly and have their efficiency limited when not combined with other techniques [6,10]. Advanced oxidation processes (AOPs) have emerged as a waste-free alternative that aid in complete mineralization of organic pollutants in aquatic media and it has reach in many cases. AOPs are characterized by the in-situ generation of highly reactive radicals (specially $^{\bullet}$OH), which are able to attack most of the recalcitrant organic pollutants [11,12]. A wide range of AOPs have been investigated in the removal of organic pollutants in these last few decades such as photoperoxidation [13], electrochemical processes [14], Fenton and electro-Fenton reactions [15,16], sonochemical-assisted processes [17,18], and heterogeneous photocatalysis [12–19].

Among a diversity of advanced oxidation mechanisms, heterogeneous photocatalysis has gained attention by employing TiO_2 [20,21], ZnO [22,23], and the combination of TiO_2 and ZnO [24]. Other photocatalyst combinations for dye degradation have been reported, such as $TiO_2/SiO_2/Fe_2O_3$ [25] and $ZnO@SiO_2$ [26]. Titanium dioxide is still the favorite in photocatalysis due to its photochemical properties and low cost, followed by ZnO, which has also demonstrated high efficiency in pollutant degradation under UV light [27]. The application of mixed materials combined with water-soluble oxidizing agents, such as hydrogen peroxide, has been recently reported as presenting synergic effects in the removal of organic pollutants [28–30]. Aquino et al. [31] have reported an enhancement in photocatalytic activity of TiO_2/UV-C by adding H_2O_2 at a certain dosage to remove green leaf dye from a water medium. Santos et al. [32] investigated the removal of Brilliant Blue FCF and erythrosine by combining H_2O_2 and immobilized TiO_2 exposed to UV-C radiation. Kumawat et al. [22] studied the removal of nigrosin, an anionic dye, by photocatalysis with doped and non-doped zinc oxide.

Organic oxidation reactions may be complex and require the application of a variety of kinetic models to fit the wide range of degradation data in order to understand the mechanisms involved in the processes. Some recent works have reported artificial neural networks (ANNs) as a promising modeling technique for AOP reactions [30,31].

ANNs are able to learn the behavior of a phenomenon when variables are studied and correlate multiple inputs to outputs; it is possible to correlate several factors, such as pH, reactants' initial concentrations, and time to obtain the concentration of pollutants under these given conditions, which is not possible with conventional phenomenological models. ANNs can be used to analyze complex chemical phenomena and reaction patterns such as the oxidation of dye molecules in water [30]. Therefore, ANN is ideal to describe complex processes not fully understood such as in this study. A lack of reports addressing the application of ANNs for the AOP treatment systems of multicomponent mixtures deserves to be highlighted, especially for pollutants from the food industry.

Thus, this work aimed to (1) evaluate the degradation of synthetic dyes such as erythrosine (ER) and Fast Green (FG) mixture samples in different AOP systems, (2) analyze the degradation data with usual kinetic models, and (3) compare these models with ANNs. For the experimental design, hydrogen peroxide (H_2O_2), titanium dioxide, and zinc oxide were employed as oxidation agents under UV-C radiation. Finally, four toxicity assays were performed in order to compare the acute toxicity of the samples before and after the treatment.

2. Experimental setup

2.1. Materials

The synthetic anionic dyes erythrosine (ER, CI 45430, $C_{20}H_6I_4Na_2O_5$) and Fast Green (FG, CI 42053, $C_{37}H_{34}N_2O_{10}S_3$) are commonly used in food industry processes. Those used in this study were purchased from F. Trajano Aromas & Ingredientes Ltda (Brazil). Titanium dioxide P-25 (80% anatase phase and 20% rutile phase, specific area of 50 m^2 g^{-1}) and ZnO (specific area of 5 m^2 g^{-1}) were acquired from Evonik Degussa Ltda. (Brazil) and Biodinâmica Química e Farmacêutica Ltda. (Brazil), respectively. Hydrogen peroxide was purchased from Peroxidos Ltda. (Brazil).

2.2. Dye degradation

Samples of 10 mg L^{-1} of each dye were prepared for the experiments. The assays were carried out with 300 mL of sample in a photocatalytic batch reactor using a UV-C lamp (ILUMISAMPA, 30 W, λ = 254 nm). The lamp was heated for 30 m to stabilize the radiation emission before each experiment and the heterogeneous systems with a solid catalyst dispersed in dye solution were pre-stirred for 30 min to dismiss the effects of adsorption onto the particles, as reported by Nascimento Júnior et al. [19]. Hydrogen peroxide concentration was 2.86 mmol L^{-1}, which corresponded to the stoichiometry amount needed to completely degrade all the dyes. Catalyst concentration was 0.33 g L^{-1}.

Different processes were compared to select which one would cause the highest degradation rates and the results are displayed in Table S1, including operational costs on a laboratory scale. Kinetic degradation assays were performed for 90 min with 4-mL sample withdrawal at 5, 15, 30, 45, 60, 75, and 90 min. After collection, the samples were centrifuged for 30 min at 3,500 rpm to separate the solid catalyst. The resulting degraded sample was analyzed in

UV-vis SPECTROQUANT PHARO 300 spectrophotometer. The wavelengths of maximum absorption occurred at 254 nm for aromatic content in dyes and 527 and 622 nm, respectively, for ER and FG. The analytical parameters for the analyses are displayed in Table S2.

3. Experimental design

A 2^3-experimental design evaluated the effects of the operational conditions on dye degradation. The parameters investigated in the study were catalyst mass (0.05, 0.1, and 0.15 g), peroxide concentration (1.67, 2.86, and 4.29 mmol L^{-1}), and pH (5, 7, and 9). The central point was performed in triplicate to determine the experimental error. Statistica Experimental Design 10© was used for data analyses. Each experiment lasted up to 120 min.

3.1. Kinetic and neural network modeling

An assay was performed using the selected conditions from the previous analyses to evaluate the temporal behavior of pollutant removal. The assays were carried out in duplicate. The non-linear pseudo-first-order (PFO) kinetic model (Eq. (1)) was fit to the concentration data using OriginPro 9.0 software.

$$\frac{[C]}{[C_0]} = e^{-kt} \tag{1}$$

An ANN model was developed based on the experimental results from experimental design assays. They were used to train the ANN model. The input data were normalized to the range [−1, 1] and the neural network structure was built with 4 input parameters, 3 neurons in the hidden layer, and 2 output parameters (type 4:3:2). The input set of data was characterized by the amount of ZnO (mg), the concentration of H$_2$O$_2$ (μL), pH, time (in minutes). The output data were generated in normalized values and taken to degradation rates of dyes ($C.C_0^{-1}$) and aromatics (Ar.Ar$_0^{-1}$). The software was developed in C# language in Unity 3D© and the adopted criteria were absolute mean error and the R^2. A feedforward network type with a sigmoidal activation function between −1 and 1 was employed according to Eq. (2). All the degradation data fed in, to a total of nine experimental conditions and 81 points. The training method used a combination of techniques such as particle swarm optimization, genetic algorithm, and random search, in order to attain a network with minimized error. The total training time lasted 7,600 s according to the requirements of stabilization of residual error.

3.2. Environmental parameters and toxicity of the degraded dyes

Chemical oxygen demand (COD) and total organic carbon (TOC) analyses were carried out for raw and post-treatment samples. COD measurements were performed as in Standard Methods for Examination of Water and Wastewater [32] while TOC measurements were accomplished in a TOC-VCPN meter (SHIMADZU Co., Japan).

Toxicity assessment of raw and treated samples was carried out with *Lactuca sativa* (lettuce) seeds according to

the methods proposed by Utzig et al. [33]. The seeds were purchased from Feltrin Sementes LTDA. (Brazil) and the negative and positive controls were made of distilled water and boric acid (3%), respectively. Germination index (GI) was calculated by the rates of germinated seeds regarding the total number of seeds and the relative growth index (RGI) was estimated by Eq. (2).

$$GI = \frac{ARS}{ARC} \tag{2}$$

where ARS is the average of root elongation when exposed to the samples and ARC is the average of root elongation when exposed to the negative control.

4. Results and discussion

4.1. Degradation of dyes using different methods

The assays performed in the absence of radiation did not reach significant dye degradation rates after 120 min. Santos et al. [32] have reported similar results in AOP systems with no UV radiation. This event indicates that the adsorption effects of catalysts and the degradation by raw oxidizing agents have minimum effect on degrading pollutants. From Fig. 1a, it is possible to observe a reasonable degradation rate (42.5%) under photolysis. This result was related to the degradation of ER; no considerable removal of FG was attained after 90 min of reaction.

The results display a slighter increase in the removal rates by employing ZnO when compared with TiO$_2$ as the photocatalyst. This can be explained by the broader range of the ZnO absorption spectrum, which facilitates the generation of radicals and maintenance of the electron–hole pair [34]. Other reports in the literature have also found superior degradation rates of dyes by employing ZnO in heterogeneous photocatalysis in comparison with TiO$_2$ [35,36]. According to the results, the best removal degradation rates were attained with the H$_2$O$_2$ and ZnO/H$_2$O$_2$ UV-C-based systems (88.9% and 92.9% after 90 min, respectively). Neves et al. [20] observed 80% of degradation removal rates for a binary textile dye sample after 150 m in a TiO$_2$/H$_2$O$_2$ UV-C-based system, while Brahim et al. [37] observed similar rates in only 60 min in a ZnO/H$_2$O$_2$ system.

Regarding the ZnO system, the presence of H$_2$O$_2$ in heterogeneous systems was demonstrated to enhance the degradation rates, corroborating the synergic effect observed in the process. As reported by Barbosa et al. [38], in addition to increasing free radicals •OH generation rates, H$_2$O$_2$ is also believed to suppress the recombination of the electron/hole pair on photocatalyst. As a consequence of that, zinc oxide is able to be longer in the excited state enhancing the efficiency of the degradation.

Fig. 1b displays the degradation results for the aromatic content in ER and FG dyes. Low degradation rates (32.0%) were obtained in the H$_2$O$_2$/UV-C, despite the high efficiency in removing color. Nascimento et al. [39] obtained a low degradation rate for aromatics in the treatment of food dyes with a photoperoxidation process under UV-C light, corroborating the results achieved in this work. The other experiments demonstrated efficiency
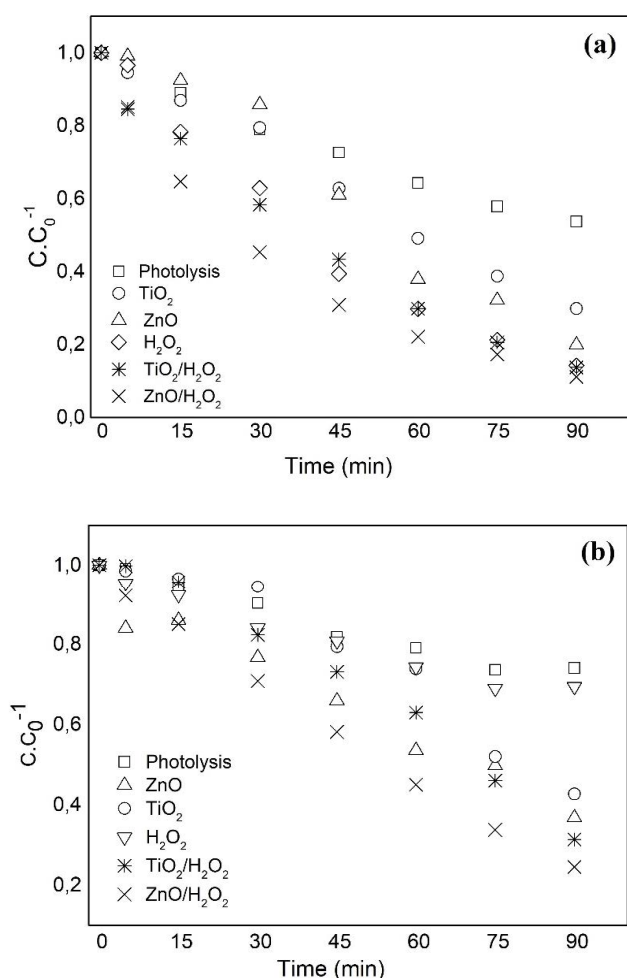
Fig. 1. Degradation kinetics of (a) ER and FG dyes and (b) aromatics for binary dyes under UV-C radiation using processes: photolysis, photocatalysis TiO_2, ZnO, H_2O_2, TiO_2/H_2O_2, ZnO/H_2O_2. $[C_0]$ = 10 mg L^{-1} each dye; $[H_2O_2]$ = 2.86 mmol L^{-1}; $[TiO_2]$ = 0.33 g L^{-1}; $[ZnO]$ = 0.33 g L^{-1}; pH = 7.

Fig. 2. Effect of variables in the (a) aromatics and (b) dye degradation with $ZnO/H_2O_2/UV$-C process.

in degrading the aromatic content, especially TiO_2/H_2O_2 and ZnO/H_2O_2, reaching 71.3% and 76.7%, respectively. Thus, the presence of photocatalysts is believed to impact positively not only the removal of color but also the aromatics. According to the results, the best performance was observed in ZnO/H_2O_2 system (93% color removal and 77% aromatics removal).

4.2. Experimental design using $ZnO/H_2O_2/UV$-C process

Statistical analysis of the previous assays was carried out from a central composite design followed by response surface methodology for data under different experimental settings. Fig. 2 presents a Pareto chart for the effect of the variables on aromatics and dye degradation using the UV-C/H_2O_2/ZnO process, with a confidence level of 95%. Fig. 2a shows that all the interactions among the parameters exhibited statistical significance. In Fig. 2b, the pH values did not present a heavy influence on the degradation rates, although interactions of pH with the other variables

did. At a low pH medium, the adsorption of ER and FG is favorable on the surface of the catalyst since these dyes are anionic in water media (pKa values of 4.1 and 3.5, respectively), and ZnO is positively charged at a pH lower than 9 [40]. When the catalyst is oppositely charged to the targeted compounds, the efficiency of removal is enhanced since the electrostatic interaction is enhanced. At high pH values, the availability of OH^- is greater, which enhances the generation of hydroxyl radicals in theory [41]. Thus, effective results for the removal of ER and FR can be observed for a range of pH values.

Peroxide concentration demonstrated a heavy positive influence on the removal rates, which indicates that the concentration used was not excessive, although H_2O_2 and ZnO were inferior to the other effects when combined. Higher concentrations of H_2O_2 favored the degradation reactions, but when excess was reached in the presence of ZnO, the incidence of radiation on the catalyst was inhibited. The concentration of the photocatalyst was not excessive, as can be seen in the results. When this is the case, the turbidity of the samples will hinder the scattering of radiation then, reducing the radical generation rate [42].

The surface response analysis (Fig. 3) displays the predicted averages of the interactions. The charts express the influence of the variables in the response variable. Results show that the parameters at intermediary levels displayed higher efficiency when compared with the range limits,

except for the chart in Fig. 3c, where the highest concentrations of hydrogen peroxide displayed higher levels of efficiency in degrading aromatic content at a lower pH. For this reason, the central level is the most adequate set of parameters for the degradation of both dyes and aromatic content.

Table 1 shows the analysis of variance (ANOVA) estimation for the interactions of the investigated parameters. According to Table 1, parameters demonstrated that the fit was suitable to predict the experimental design at different levels within the investigated range since $R^2 > 0.96$ and pure error was minimal. The influence of pH and its interactions did not present statistical significance in the degradation of the aromatics and dyes ($p > 0.05$). For color removal, it is possible to observe that the interactions between ZnO and pH, and H_2O_2 and pH were not statistically significant; however, the interaction between ZnO and

H_2O_2 statistically altered the color and aromatics removal ($p < 0.05$).

Statistical analysis also provided an empirical linear model for the aromatics removal rate [Eq. (3)] and color [Eq. (4)] from the linear regression coefficients. The model describes the percentage removal D (%) according to the statistical significance of the variables and interactions studied.

$$D_{\text{aromatics}}\left(\%\right) = 78.62 + 16.72X_{[\text{ZnO}]} + 5.52X_{[\text{H}_2\text{O}_2]}$$
$$- 4.52_{[\text{ZnO}]}X_{[\text{H}_2\text{O}_2]} + 11.47X_{[\text{ZnO}]}X_{\text{pH}} + 4.52X_{[\text{H}_2\text{O}_2]}X_{\text{pH}}$$
$$- 57.56X_{[\text{ZnO}]}X_{[\text{H}_2\text{O}_2]}X_{\text{pH}} \tag{3}$$

$$D_{\text{color}}\left(\%\right) = 96.63 + 7.40X_{[\text{ZnO}]} + 8.75X_{[\text{H}_2\text{O}_2]}$$
$$- 5.20X_{[\text{ZnO}]}X_{[\text{H}_2\text{O}_2]} - 19.82X_{[\text{ZnO}]}X_{[\text{H}_2\text{O}_2]}X_{\text{pH}} \tag{4}$$
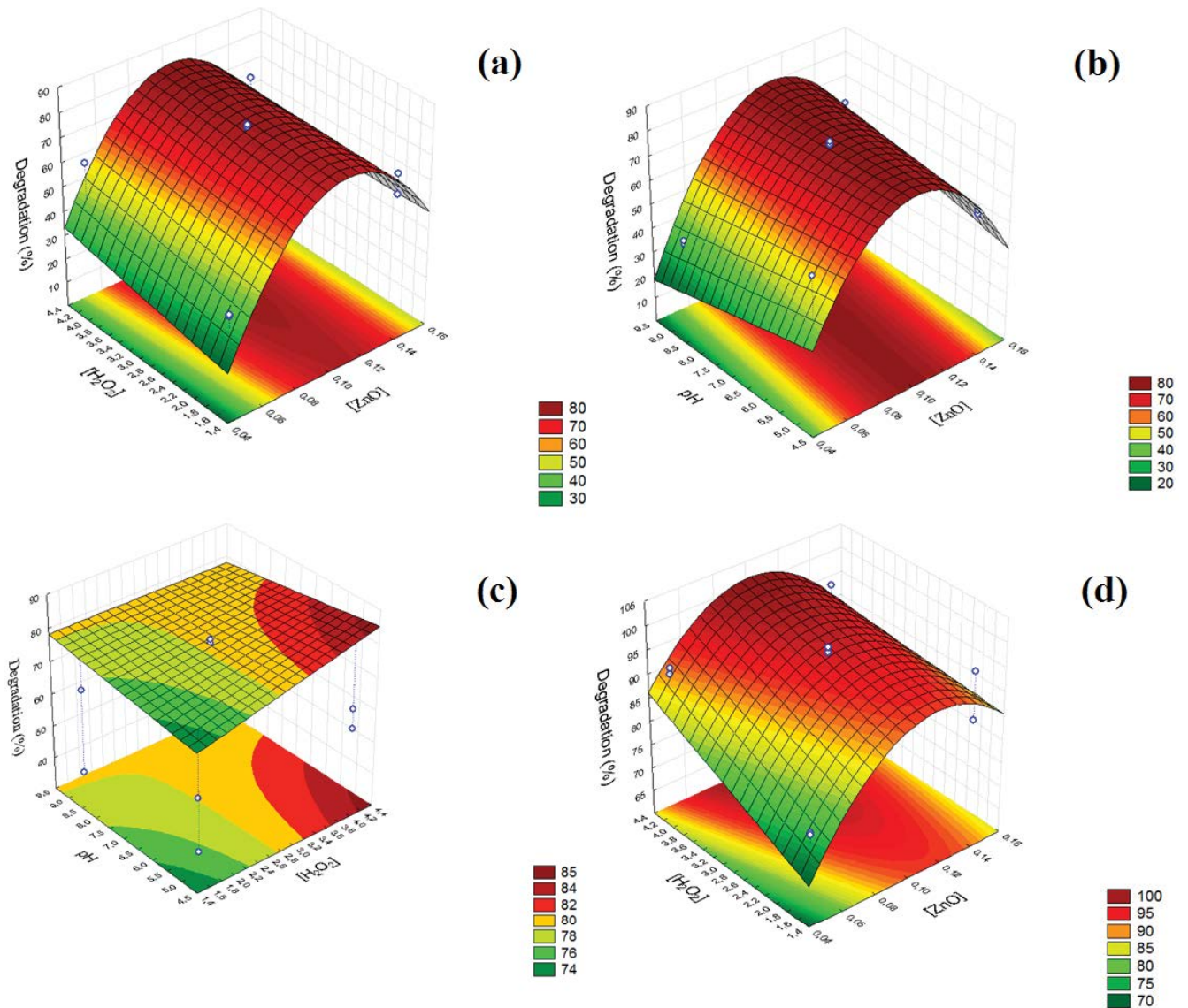
Fig. 3. Response surfaces of aromatics degradation: (a) [ZnO] × [H_2O_2], (b) [ZnO] × pH, (c) [H_2O_2] × pH and ER and FG dyes degradation, and (d) [ZnO] × [H_2O_2].

Table 1
Analysis of variance (ANOVA) for interactions of the parameters in aromatics and dye degradation

Factor	Aromatics		Dyes	
	F	$p*$	F	$p*$
[ZnO]	17.28873	0.00104	47.54848	0.02039
[H_2O_2]	1.88667	0.00032	66.47974	0.01471
pH	0.02816	0.33778	9.17149	0.09392
[ZnO] × [H_2O_2]	1.26552	0.01395	23.47902	0.04005
[ZnO] × pH	8.13835	0.00221	11.88712	0.07481
[H_2O_2] × pH	1.26552	0.01395	3.64906	0.19628
R^2	0.966		0.988	
Pure error	0.583		2.303	

*The interactions, which were not significant at a 95% confidence level, are in bold.

In addition, the best degradation removal rate (98.29%) was attained when the experiment was performed in the central point condition, which is highlighted in Table S3. Thus, this condition was selected for further kinetic evaluation.

4.3. Kinetic study and neural network modeling

From the removal kinetic investigation, it is possible to determine reaction rate, one of the most important parameters in chemical processes [43,44]. Fig. 4 displays the kinetic profile and the PFO kinetic model fitted to the data. According to the kinetic data, 50% of dye degradation removal was attained within the first 30 min and 91% after 90 min. For aromatic content, 70% had been degraded and removed by the end of the experiment. Samarghandi et al. [4] found 89.3% removal rates of acid red 14 ($C_0 = 100$ mg L^{-1}) by using UV radiation, H_2O_2, and zerovalent iron (nZVI). Rahmani et al. [45] attained 99.8% removal of acid blue 113 in an AOP-based electro/persulfate system.

The PFO kinetic model was fit to the data. The kinetic rate constant was in the order of 0.0266 ± 0.0003 m^{-1} for dye degradation and 0.0127 ± 0.0005 m^{-1} for aromatics degradation. As exhibited in Fig. 4a, the fitting was suitable with R^2 calculated at 0.986 and 0.999 for aromatic and dye removals, respectively, which points out to a first-order reaction.

The PFO model assumes a reaction rate that depends only on the dye concentration, considering an excess of H_2O_2 [19]. Many reports have suggested that advanced oxidation systems follow a first-order reaction to synthetic dye aqueous solutions, including systems with solid photocatalysts and oxidizing agents [30,31]. Tekin et al. [46] employed bismuth oxyhalide as a photocatalyst in the photo-Fenton reaction to remove tartrazine food dye from water with a 0.0027 m^{-1} kinetic rate at 30°C according to PFO modeling. Barbosa et al. [38] found a 0.0208 m^{-1} rate constant in removing Bordeaux red and tartrazine in binary systems in the TiO_2/H_2O_2 AOP system and attained 97% of color removal in 180 min. The sum of the fitting residual squares (Fig. 4b) was estimated at 0.0084 and 0.0007 for aromatics and dyes, respectively, similar to the results

(a)

(b)
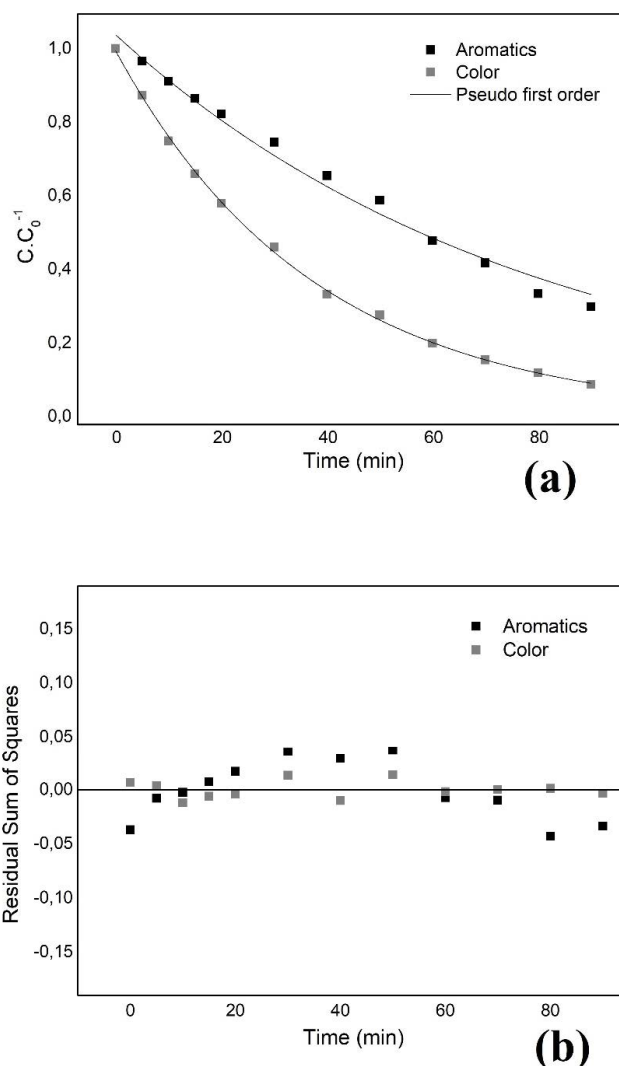
Fig. 4. (a) Pseudo-first-order kinetic fitting and (b) residual error of degradation of dyes and aromatics in ZnO/H_2O_2 system (mZnO = 100 mg; [H_2O_2] = 2.86 mmol L^{-1}; pH = 7.0).

achieved by Santos et al. [32] in the degradation of erythrosine and Brilliant Blue samples. The low residual error indicates that the PFO model is appropriate to describe the concentration profile.

Table 2 displays other results reported in the literature that investigated the photocatalytic degradation of synthetic food dyes by H_2O_2 and ZnO. These studies indicate that dye degradation could be easily attained even for single-dye samples. Low reaction times at neutral pH are another advantage of the process since these results aid feasibility for scaling-up projects.

The ANNs model for the degradation training data is exhibited in Fig. 5. The network parameters are represented by the weights and biases. The model was able to predict the concentration of dyes and aromatics concentration as output.

According to Fig. 5a, the network normalized the set of data in the range of [0,150] to [–1,1] for the input, and

Table 2
Background of the degradation of food dyes by ZnO and H_2O_2 photocatalysis

Food dye	$[H_2O_2]$ (mM)	[ZnO] (g L^{-1})	pH	Dye degradation (%)	Time (min)	Reactant costs* (US$.m^{-3})	References
Acid Orange 7	12	0.16	7	80	20	25.2	[28]
Azophloxine	8	1.5	6	60	180	223.1	[29]
Tartrazine/Fast Green	9.8	–	7.2	70	240	0.3	[31]
Brilliant Blue/Erythrosine	11.2	–	6.5	92	240	0.4	[32]
Sunset Yellow/Tartrazine	1.5	–	5.5	90	120	0.04	[39]
Tartrazine	–	0.2	6	95	120	29.8	[47]
Tartrazine	–	0.1	6	60	90	14.9	[48]
Erythrosine Indigotine	147	2	5.3	80	60	303.2	[49]
				85			
Erythrosine/Fast Green	2.8	0.33	7	98	120	50.1	This work

*H_2O_2 cost: $5.47/gallon; ZnO cost: $149/kg (according to the Independent Commodity Intelligence Services e Inframat Advanced Materials).
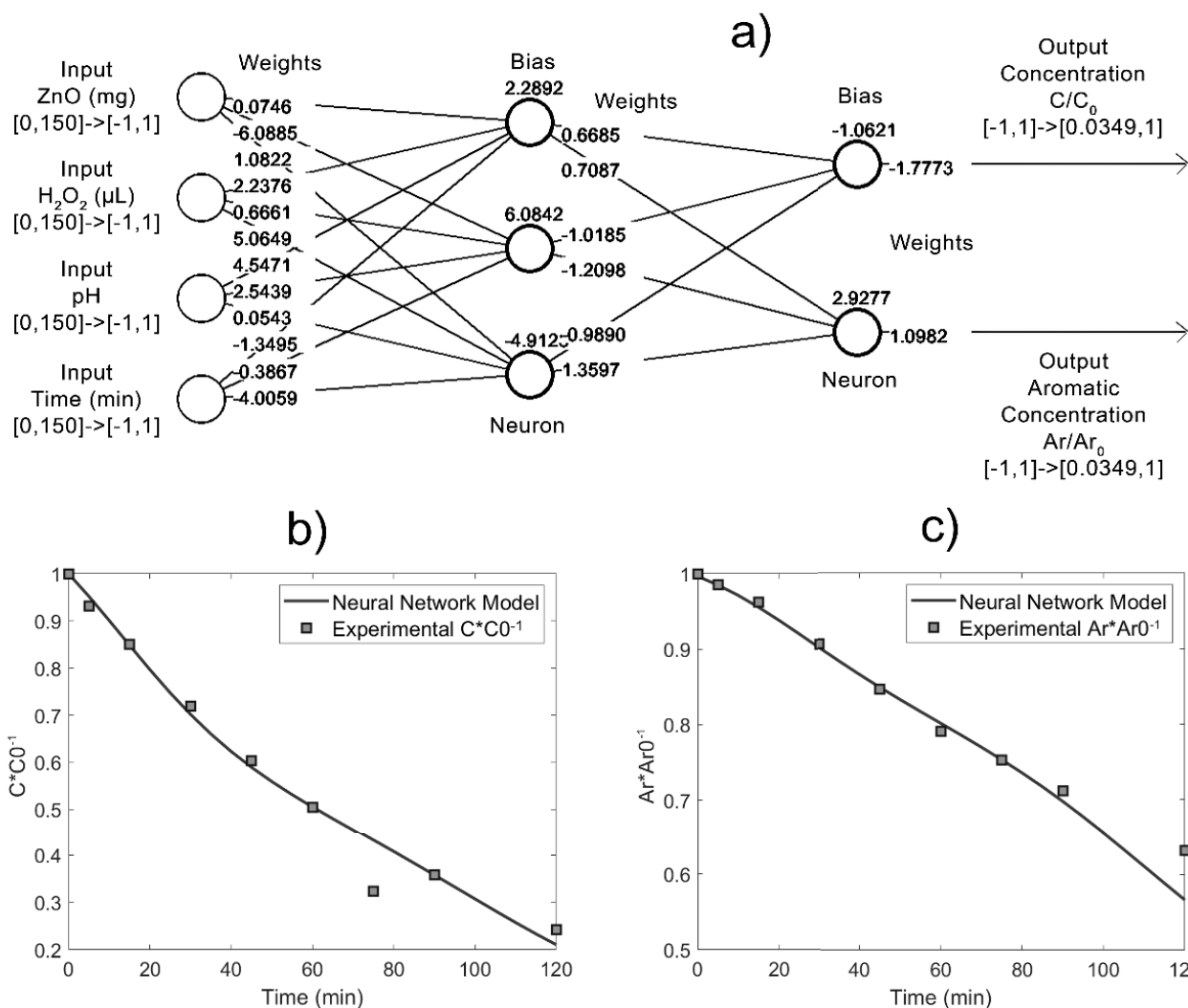
Fig. 5. (a) Artificial neural network model for the degradation in the ZnO/H_2O_2/UV-C system, (b) erythrosine and Fast Green dyes mixture, and (c) aromatics from the dyes. ZnO (50 mg)/H_2O_2 (34 μL)/pH(5)/UV-C.

Table 3
Germination index (GI) and relative growth index (RGI) for dye sample before and after 120 min degradation using ZnO/H$_2$O$_2$/UV-C process

Sample	Germination index (%)	Average root growth (cm)	Relative growth index
Negative control	96.7 ± 1.2	1.81 ± 0.10	–
Before degradation	72.6 ± 2.5	1.16 ± 0.26	0.64
After degradation	90.0 ± 2.8	1.54 ± 0.14	0.85

as the output in the range of [–1,1] to [0.0349,1]. This aims to decrease error margins. The calculation of the resulting ANN may be executed in any software by 3-part pseudo-code (input normalizing, network calculation, and output denormalization), as presented in Supplementary material.

Fig. 5b and c demonstrate the correlation between the ANN model and experimental data for one set of experimental parameters. Similar behavior was observed in the simulation of other reaction conditions. The average error was estimated at 0.025 and the correlation coefficient at 0.978. The neural network model is more general and broad in applicability because several factors are included in the model, such as pH, quantities of ZnO and H$_2$O$_2$, variables that are not possible to be comprised by the PFO kinetics. Due to the high differences in ANN structures and central composite design (CCD), such as strong non-linearity in ANNs and the use of many parameters, it is not possible to compare both once a polynomial model as CCD would be too simple to pair with ANNs. ANNs can interpolate, generalize and extrapolate better than an experimental design model as stated by Amato et al. [50]. For all these reasons, it can be considered that the application of ANN to model the degradation kinetic of erythrosine and Fast Green dyes and aromatics in a ZnO/H$_2$O$_2$/UV-C photocatalytic process as an adequate tool to simulate the process and design an enlarged-scale reactor.

4.4. Environmental parameters and toxicity assays

TOC and COD measurements were performed in raw samples and water treated in ZnO/H$_2$O$_2$/UV-C under the selected operating conditions. TOC measurements shrunk from 64.3 to 34.6 mg L^{-1}, which represents a 45% reduction of organic carbon. Regarding COD, removal was estimated at 58.2% falling from 174.5 to 72.8 mgO$_2$ L^{-1} after the oxidation process. These results represent a considerable reduction in dissolved organic matter and partial mineralization of the AOP process in binary samples. Aquino et al. [31] found 66%, 73%, and 98% removal rates for TOC, COD, and color, respectively, when treating a binary sample with tartrazine and FG by TiO$_2$/H$_2$O$_2$/UV-C for 240 min. Tekin et al. [46] treated tartrazine by employing metal-doped BiOCl in visible-light-assisted Fenton reaction and attained 59% of TOC removal and 95% of color removal in 90 min. Other research also points out the efforts needed to achieve partial TOC removal, indicating the presence of organic by-products besides inorganic ions and CO$_2$.

The GI and RGI values for raw dye samples and after 120 min degradation are exhibited in Table 3. The positive control inhibited the growth of 100% of the seeds as expected.

According to Table 2, the negative control displayed high GI as well as root elongation rates. For the samples prepared with raw dyes, these values were considerably lower. According to Luo et al. [49], when GI is superior to 80% it indicates that no significant toxicity has been inflicted by the samples. According to the results, the treated samples did not present severe effects on the germination of lettuce seeds. Regarding the growth of the roots, inhibitory effects are in the range of 0 < RGI > 0.8, no significant effects 0.8 < RGI < 1.2, and stimulative effects in RGI > 1.2 [33]. The results displayed in Table 2 imply that the by-products in the degraded dye solution (inorganic ions and possible small organic molecules) did not inhibit the growth of the lettuce roots, differently from the raw samples. The decrease in acute toxicity can be observed in some other reports in the literature [31,32–51] with the use of lettuce seeds, corroborating the efficacy of the treatment.

5. Conclusions

This work showed that photodegradation of erythrosine and Fast Green presented high degradation rates in a ZnO/H$_2$O$_2$/UV-C system, compared with TiO$_2$/H$_2$O$_2$/UV-C. An experimental design indicated the best operational conditions ([H$_2$O$_2$] = 2.8 mM, [ZnO] = 0.33 g L^{-1}, pH 7), reaching up to 98% of degradation rates after 120 min. Kinetic modeling of the degradation of dyes using the ZnO/H$_2$O$_2$/UV-C process under the best operational condition well fitted the PFO model. Artificial neural networks can develop a more general model to represent experimental kinetic data, making this an alternative modeling technique for describing AOP process efficiency. Toxicity tests via germination and relative growth index of *Lactuca sativa* seeds demonstrated a reduction of the inhibition effects after the process of the degradation of the dyes. The degradation of a solution of food dye mixtures via heterogeneous photocatalysis demonstrated a reduction in toxicity, indicating that this chemical oxidation process represents an encouraging method for the pre-treatment of conventional effluent treatment processes in the food industry.

References

[1] C.H. Nguyen, R.-S. Juang, Efficient removal of cationic dyes from water by a combined adsorption-photocatalysis process using platinum-doped titanate nanomaterials, J. Taiwan Inst. Chem. Eng., 99 (2019) 166–179.

[2] M. Roosta, M. Ghaedi, A. Daneshfar, R. Sahraei, A. Asghari, Optimization of combined ultrasonic assisted/tin sulfide nanoparticle loaded on activated carbon removal of erythrosine by response surface methodology, J. Ind. Eng. Chem., 21 (2015) 459–469.

[3] M.O. Dawodu, K.G. Akpomie, Evaluating the potential of a Nigerian soil as an adsorbent for tartrazine dye: isotherm, kinetic and thermodynamic studies, Alexandria Eng. J., 55 (2016) 3211–3218.

[4] M.R. Samarghandi, A. Dargahi, H.Z. Nasab, E. Ghahramani, S. Salehi, Degradation of azo dye Acid Red 14 (AR14) from aqueous solution using H_2O_2/nZVI and $S_2O_8^{2-}$/nZVI processes in the presence of UV irradiation, Water Environ. Res., 92 (2020) 1173–1183.

[5] S. Hisaindee, M.A. Meetani, M.A. Rauf, Application of LC-MS to the analysis of advanced oxidation process (AOP) degradation of dye products and reaction mechanisms, TrAC, Trends Anal. Chem., 49 (2013) 31–44.

[6] A. Peyghami, A. Moharrami, Y. Rashtbari, S. Afshin, M. Vosuoghi, A. Dargahi, Evaluation of the efficiency of magnetized clinoptilolite zeolite with Fe_3O_4 nanoparticles on the removal of basic violet 16 (BV16) dye from aqueous solutions, J. Dispersion Sci. Technol., (2021) 1947847, doi: 10.1080/01932691.2021.1947847.

[7] K. Hasani, M. Moradi, S.A. Mokhtari, H. Sadeghi, A. Dargahi, M. Vosoughi, Degradation of basic violet 16 dye by electro-activated persulfate process from aqueous solutions and toxicity assessment using microorganisms: determination of by-products, reaction kinetic and optimization using Box–Behnken design, Int. J. Chem. React. Eng., 19 (2021) 261–275.

[8] M.R. Samarghandi, A. Dargahi, A. Shabanloo, H.Z. Nasab, Y. Vaziri, A. Ansari, Electrochemical degradation of methylene blue dye using a graphite doped PbO_2 anode: optimization of operational parameters, degradation pathway and improving the biodegradability of textile wastewater, Arabian J. Chem., 13 (2020) 6847–6864.

[9] T. Rasheed, M. Bilal, H.M.N. Iqbal, H. Hu, X. Zhang, Reaction mechanism and degradation pathway of rhodamine 6G by photocatalytic treatment, Water Air Soil Pollut., 228 (2017) 291–301.

[10] S. Kaur, S. Sharma, A. Umar, S. Singh, S.K. Mehta, S.K. Kansal, Solar light driven enhanced photocatalytic degradation of brilliant green dye based on ZnS quantum dots, Superlattices Microstruct., 103 (2017) 365–375.

[11] B. Costa-Angulo, J. Lara-Ramos, J. Diaz-Angulo, M.A. Mueses, F. Machuca-Martínez, Mechanistic model and optimization of the diclofenac degradation kinetic for ozonation processes intensification, Water, 13 (2021) 1670–1693.

[12] M.L.A. Ramalho, V.S. Madeira, I.L.O. Brasileiro, P.C. Fernandes, C.B. Barbosa, S. Arias, J.G.A Pacheco, Synthesis of mixed oxide Ti/Fe_2O_3 as solar light-induced photocatalyst for heterogeneous photo-Fenton like process, J. Photochem. Photobiol., A, 404 (2021) 112873, doi: 10.1016/j.jphotochem.2020.112873.

[13] A. Dargahi, M. Pirsaheb, S. Hazrati, M. Fazlzadehdavil, R. Khamutian, T. Amirian, Evaluating efficiency of H_2O_2 on removal of organic matter from drinking water, Desal. Water Treat., 54 (2015) 1589–1593.

[14] A. Rahmani, M. Leili, A. Seid-Mohammadi, A. Shabanloo, A. Ansari, D. Nematollahi, S. Alizadeh, Improved degradation of diuron herbicide and pesticide wastewater treatment in a three-dimensional electrochemical reactor equipped with PbO_2 anodes and granular activated carbon particle electrodes, J. Cleaner Prod., 322 (2021) 129094, doi: 10.1016/j.jclepro.2021.129094.

[15] K. Hasani, S. Hosseini, H. Gholizadeh, A. Dargahi, M. Vosoughi, Enhancing the efficiency of electrochemical, Fenton, and electro-Fenton processes using SS316 and SS316/β-PbO_2 anodes to remove oxytetracycline antibiotic from aquatic environments, Biomass Convers. Biorefin., (2021) 1–18, doi: 10.1007/s13399-021-01967-z.

[16] M.R. Samarghandi, J. Mehralipour, G. Azarian, K. Godini, A. Shabanlo, Decomposition of sodium dodecylbenzene sulfonate surfactant by electro/Fe^{2+}-activated persulfate process from aqueous solutions, Global NEST J., 19 (2017) 115–121.

[17] A.R. Rahmani, A. Shabanloo, M. Fazlzadeh, Y. Poureshgh, M. Vanaeitabar, Optimization of sonochemical decomposition of ciprofloxacin antibiotic in US/PS/nZVI process by CCD-RSM method, Desal. Water Treat., 145 (2019) 300–308.

[18] A. Dargahi, H.R. Barzoki, M. Vosoughi, S.A. Mokhtari, Enhanced electrocatalytic degradation of 2,4-dinitrophenol (2,4-DNP) in three-dimensional sono-electrochemical (3D/SEC) process equipped with Fe/SBA-15 nanocomposite particle electrodes: degradation pathway and application for real wastewater, Arabian J. Chem., 15 (2022) 103801, doi: 10.1016/j.arabjc.2022.103801.

[19] W.J. Do Nascimento Júnior, R.V.S. Aquino, A.A. Barbosa, O.R. Rocha, Development of a new PET flow reactor applied to food dyes removal with advanced oxidative processes, J. Water Process Eng., 31 (2019) 100283, doi: 10.1016/j.jwpe.2019.100823.

[20] N.S.C.S. Neves, A.A. Barbosa, I.L.S. Santana, P.M.N. Pereira, J.G.A. Pacheco, M. Benachour, O.R.S. Rocha, Treatment of bicomponent textile dyes using combined photocatalysis and adsorption process made from residue-based reactor and adsorbent material, Chem. Eng. Commun., 208 (2020) 1523–1542.

[21] L.N. Ribeiro, A.C. Fonseca, E.F. Silva, E.D. Oliveira, A.T. Ribeiro, L.C. Maranhão, J.G.A. Pacheco, G. Machado, L.C. Almeida, Residue-based TiO_2/PET photocatalytic films for the degradation of textile dyes: a step in the development of green monolith reactors, Chem. Eng. Process., 147 (2020) 107792–107800.

[22] S. Kumawat, K. Meghwal, S. Kumar, R. Ameta, C. Ameta, Kinetics of sonophotocatalytic degradation of an anionic dye nigrosine with doped and undoped zinc oxide, Water Sci. Technol., 80 (2019) 1466–1475.

[23] S.M. Mirmousaei, M. Peyravi, M. Khajouei, M. Jahanshahi, S. Khalili, Preparation and characterization of nano-filtration and its photocatalytic abilities via pre-coated and self-forming dynamic membranes developed by ZnO, PAC and chitosan, Water Sci. Technol., 80 (2019) 2273–2283.

[24] R.D. Shinde, P.S. Tambade, M.G. Chaskar, K.M. Gayade, Photocatalytic degradation of dyes in water by analytical reagent grades ZnO, TiO_2 and SnO_2: a comparative study, Drinking Water Eng. Sci., 10 (2017) 109–117.

[25] S. Behzadi, B. Nonahal, S.J. Royaee, A.A. Asadi, TiO_2/SiO_2/Fe_3O_4 magnetic nanoparticles synthesis and application in methyl orange UV photocatalytic removal, Water Sci. Technol., 82 (2020) 2432–2445.

[26] X. Shen, Y. Shi, H. Shao, Y. Liu, Y. Zhai, Synthesis and photocatalytic degradation ability evaluation for rhodamine B of ZnO@SiO_2 composite with flower-like structure, Water Sci. Technol., 80 (2019) 1986–1995.

[27] Z. Youssef, L. Colombeau, N. Yesmurzayeva, F. Baros, R. Vanderesse, T. Hamieh, J. Toufaily, C. Frochot, T. Roques-Carmes, S. Acherar, Dye-sensitized nanoparticles for heterogeneous photocatalysis: cases studies with TiO_2, ZnO, fullerene and graphene for water purification, Dyes Pigm., 159 (2018) 49–71.

[28] N. Daneshvar, S. Aber, F. Hosseinzadeh, Study of C.I. Acid Orange 7 removal in contaminated water by photo oxidation processes, Global NEST J., 10 (2008) 16–23.

[29] V. Anand, V.C. Srivastava, Photocatalytic degradation of nitrobenzene and azo dye using nanoparticles prepared by electrochemical method, J. Sci. Ind. Res., 75 (2016) 632–637.

[30] A.A. Barbosa, R.V.S. Aquino, N.S.C.S. Neves, R.F. Dantas, M.M.M.B. Duarte, O.R.S. Rocha, Kinetic study of dye removal using TiO_2 supported on polyethylene terephthalate by advanced oxidation processes through neural networks, Water Sci. Technol., 79 (2019) 1134–1143.

[31] R.V.S. Aquino, A.A. Barbosa, L.B. Ribeiro, A.F.B. Oliveira, J.P. Silva, P.M. Azoubel, O.R.S. Rocha, Degradation of leaf green dye by heterogeneous photocatalysis with TiO_2 over a polyethylene terephthalate plate, Chem. Pap., 73 (2019) 2501–2512.

[32] S.C. Lenore, E.G. Arnold, D.E. Andrew, Standard Methods for the Examination of Water and Wastewater, American Public Health Association, New York, 1998.

[33] L.M. Utzig, R.M. Lima, M.F. Gomes, W.A. Ramsdorf, L.R.R. Martins, M.V. Liz, A.M. Freitas, Ecotoxicity response of chlorpyrifos in *Aedes aegypti* larvae and *Lactuca sativa* seeds

after UV/H₂O₂ and UVC oxidation, Ecotoxicol. Environ. Saf., 169 (2019) 449–456.

[34] D. Štrbac, C.A. Aggelopoulos, G. Štrbac, M. Dimitropoulos, M. Novaković, T. Ivetić, S.N. Yannopoulos, Photocatalytic degradation of naproxen and methylene blue: comparison between ZnO, TiO₂ and their mixture, Process Saf. Environ. Prot., 113 (2018) 174–183.

[35] C.A. Aggelopoulos, M. Dimitropoulos, A. Govatsi, L. Sygellou, C.D. Tsakiroglou, S.N. Yannopoulos, Influence of the surface-to-bulk defects ratio of ZnO and TiO₂ on their UV-mediated photocatalytic activity, Appl. Catal., B, 205 (2017) 292–301.

[36] D. Tassalit, S. Lebouachera, S. Dechir, N. Chekir, O. Benhabiles, F. Bentahar, Comparison between TiO₂ and ZnO photocatalytic efficiency for the degradation of tartrazine contaminant in water, Int. J. Environ. Sci., 1 (2016) 357–364.

[37] I.O. Brahim, M. Belmedani, H. Hadoun, A. Belgacem, The photocatalytic degradation kinetics of food dye in aqueous solution under UV/ZnO system, React. Kinet. Mech. Catal., 133 (2021) 1075–1095.

[38] A.A. Barbosa, R.V.S. Aquino, M.G. Silva, W.J. Nascimento Júnior, M.M.M.B. Duarte, R.F. Dantas, O.R.S. Rocha, New aluminum mesh from recyclable material for immobilization of TiO₂ in heterogeneous photocatalysis, Can. J. Chem. Eng., 98 (2020) 1124–1138.

[39] G.E. Nascimento, V.O.M. Cavalcanti, R.M.R. Santana, D.C.S. Sales, J.M. Rodríguez-Díaz, D.C. Napoleão, M.M.M.B. Duarte, Degradation of a sunset yellow and tartrazine dye mixture: optimization using statistical design and empirical mathematical modeling, Water Air Soil Pollut., 231 (2020) 254, doi: 10.1007/s11270-020-04547-5.

[40] K.M. Lee, C.W. Lai, K.S. Ngai, J.C. Juan, Recent developments of zinc oxide based photocatalyst in water treatment technology: a review, Water Res., 88 (2016) 428–448.

[41] M.M. Uddin, M.A. Hasnat, A.J.F. Samed, R.K. Majumdar, Influence of TiO₂ and ZnO photocatalysts on adsorption and degradation behaviour of erythrosine, Dyes Pigm., 75 (2007) 207–212.

[42] P. Bansal, N. Bhullar, D. Sud, Studies on photodegradation of malachite green using ZnO/TiO₂ photocatalyst, Desal. Water Treat., 12 (2009) 108–113.

[43] M.M. Mahmoudi, R. Khaghani, A. Dargahi, G.M. Tehrani, Electrochemical degradation of diazinon from aqueous media using graphite anode: effect of parameters, mineralisation, reaction kinetic, degradation pathway and optimisation using central composite design, Int. J. Environ. Anal. Chem., 102 (2020) 1–26.

[44] A. Seid-Mohammadi, G. Asgarai, Z. Ghorbanian, A. Dargahi, The removal of cephalexin antibiotic in aqueous solutions by ultrasonic waves/hydrogen peroxide/nickel oxide nanoparticles (US/H₂O₂/NiO) hybrid process, Sep. Sci. Technol., 55 (2019) 1–11.

[45] A.R. Rahmani, A. Shabanloo, M. Fazlzadeh, Y. Poureshgha, H. Rezaeivahidian, Degradation of Acid Blue 113 in aqueous solutions by the electrochemical advanced oxidation in the presence of persulfate, Desal. Water Treat., 59 (2017) 202–209.

[46] G. Tekin, G. Ersöz, S. Atalay, Visible light assisted Fenton oxidation of tartrazine using metal doped bismuth oxyhalides as novel photocatalysts, J. Environ. Manage., 228 (2018) 441–450.

[47] A. Navid, A.A. Parviz, T.M. Saber, H.S. Waqif, D. Maher, P. Sanaz, Synthesis of ZnO-nanoparticles by microwave assisted sol-gel method and its role in photocatalytic degradation of food dye tartrazine (Acid Yellow 23), Int. J. Nano Dimens., 8 (2017) 241–249.

[48] R.A. Devi, B. Kavitha, M. Rajarajan, A. Suganthi, An eco-friendly highly stable and efficient NiC-S codoped wurtzite ZnO nanoplate: a smart photocatalyst for the quick removal of food dye under solar light irradiation, Sep. Sci. Technol., 53 (2018) 2456–2467.

[49] Y. Luo, J. Liang, G. Zeng, M. Chen, D. Mo, G. Li, D. Zhang, Seed germination test for toxicity evaluation of compost: its roles, problems and prospects, Waste Manage., 71 (2018) 109–114.

[50] F. Amato, J.L. González-Hernández, J. Havel, Artificial neural networks combined with experimental design: a "soft" approach for chemical kinetics, Talanta, 93 (2012) 72–78.

[51] A.R.S. Feliciano, A.L.A. Lucena, R.M.R. Santana, L.E.M.C. Zaidan, P.M. Silva, T.H. Napoleão, M.M.M.B. Duarte, D.C. Napoleão, Advanced oxidation processes employment for the degradation of lamivudine: kinetic assessment, toxicity study and mathematical modeling, Water Qual. Res. J., 55 (2020) 249–260.

Supporting information

Computational ANN 3-part pseudocode (input normalizing, network calculation, and output denormalization), for predicting the concentration of dyes and aromatics:

```
//Normalization
Input(i) = 2 * (Input(i) – (0))/150 – 1;
//Network Computation
Output(1) = –1.777336 * (2/(1 + exp(–1 * (0.668507 * (2/(1 + exp(–1 * (0.07462409 * Input(1)–6.088518 * Input(2) + 1.082241 *
Input(3) + 2.237552 * Input(4) + 2.289237))) – 1) + 0.708703 * (2/(1 + exp(–1 * (0.6660598 * Input(1) + 5.064867 * Input(2) +
4.547126 * Input(3) + 2.543926 * Input(4) + 6.08423))) – 1) – 1.01852 * (2/(1 + exp(–1 * (0.05432883 * Input(1) – 1.349536 *
Input(2) – 0.3866765 * Input(3) – 4.005919 * Input(4) – 4.912257))) – 1) – 1.062143))) – 1);
```

Table S1
Operation costs on a laboratory scale for the AOP-based processes investigated in this study

AOP	Power costs[a] (US\$·m⁻³)	Reactant costs[b] (US\$·m⁻³)	Total operation costs (US\$·m⁻³)
UV-C	2.5	–	2.5
UV-C/H₂O₂	2.5	0.2	2.7
UV-C/TiO₂	2.5	136.7	139.2
UV-C/ZnO	2.5	50.1	52.6
UV-C/H₂O₂/TiO₂	2.5	136.8	139.3
UV-C/H₂O₂/ZnO	2.5	50.3	52.8

[a]Power costs include radiation from UV-C lamp (30 W) and magnetic stirring (5 W) (1 kWh = \$0.11).
[b]Operation conditions were considered: 120 min, 2.86 mmol L⁻¹ of H₂O₂ (\$5.47/gallon), 0.33 g L⁻¹ of TiO₂ (\$410/kg) and ZnO (\$149/kg).

Output(2) = 1.098158 * (2/(1 + exp(–1 * (–1.209849 * (2/(1 + exp(–1 * (0.07462409 * Input(1) – 6.088518 * Input(2) + 1.082241 * Input(3) + 2.237552 * Input(4) + 2.289237))) – 1) – 0.9890119 * (2/(1 + exp(–1 * (0.6660598 * Input(1) + 5.064867 * Input(2) + 4.547126 * Input(3) + 2.543926 * Input(4) + 6.08423))) – 1) + 1.35969 * (2/(1 + exp(–1 * (0.05432883 * Input(1) – 1.349536 * Input(2) – 0.3866765 * Input(3) – 4.005919 * Input(4) – 4.912257))) – 1) + 2.927677))) – 1);
//Denormalization
Output(i) = 0.48257 * Output(i) + 0.51743;

Table S2
Parameters for the analyses of ER and FG in UV-vis spectrophotometer

Parameter	ER	FG
Limit of detection (mg L⁻¹)	0.03	0.05
Limit of quantification (mg L⁻¹)	0.10	0.12
Regression coefficient (R^2)	0.998	0.999
Variance (%)	0.6	0.3

Table S3
Independent variables and response for dyes and aromatics for the factorial planning 2^3

Experiment	ZnO concentration (g L⁻¹)	H_2O_2 concentration (mmol L⁻¹)	pH	Degradation (%)	
				Aromatics	Dyes
1	0.15	4.29	9	65.3	94.1
2	0.15	4.29	5	52.1	90.3
3	0.15	1.67	9	61.9	93.7
4	0.05	4.29	9	34.7	89.3
5	0.05	4.29	5	58.3	90.7
6	0.05	1.67	9	36.1	76.3
7	0.15	1.67	5	53.5	83.6
8	0.05	1.67	5	36.8	75.8
9	0.1	2.86	7	77.7	96.5
10	0.1	2.86	7	78.2	94.6
11	0.1	2.86	7	79.2	97.6